Self-Consistent-Field Calculation of the Geometry of Protonated Cyclopropane

J. D. Petke and J. L. Whitten[1]

Contribution from the Department of Chemistry, Michigan State University, East Lansing, Michigan 48823. *Received December 7, 1967*

Abstract: Accurate SCF–MO calculations performed on protonated cyclopropane, $C_3H_7^+$, show that the ion is stable in the gas phase relative to C_3H_6 and that the equilibrium geometry corresponds to that of an edge-protonated species in which the proton is attached to the ring by a bridged hydrogen bond. Bonding is due principally to an interaction of the proton with in-plane carbon 2p orbitals of the 3e′ molecular orbital of cyclopropane. This configuration is preferred over a face-protonated geometry involving bonding to the $2p_z$ orbitals above the ring. Electronic interaction is most favorable for carbon nuclei in a 60° cyclopropane configuration, but the increase in nuclear repulsion due to the proton causes a ring opening to approximately 80° for maximum stability.

Current interest in protonated cyclopropane, $C_3H_7^+$, lies in areas of mass spectroscopy and reaction mechanism. In the former, it is well known that hydrocarbon spectra frequently show large amounts of $C_3H_7^+$,[2] a species which is thought to be exceptionally stable. Some question has existed concerning the structure of this ion. Since the appearance potential of $C_3H_7^+$ in the spectra of *n*-alkanes and isoalkanes is the same, it was originally assumed that ions from both sources had the same isopropyl structure.[3] A comparison of the ionization potential of the isopropyl radical with the appearance potential of the mass spectral $C_3H_7^+$ suggests that the two species are not the same, however, and, to resolve the anomaly, a protonated cyclopropane ring structure has been proposed for the ion.[4] Such a structure also explains the presence of CH_2D^+ in the spectra of propane-2-*d*, *n*-butane-2-*d*, and isobutane-2-*d* as a result of a rearrangement of $C_3H_7^+$ to give CH_3^+ and ethylene.[5]

Further evidence for the existence of protonated cyclopropane is found in studies of the solvolysis of cyclopropane in deuteriosulfuric acid[6] and the deamination of *n*-propylamine[7,8] where results indicate that both reactions proceed through the formation of a bridged hydrogen protonated cyclopropane intermediate. A reaction mechanism involving a similar bridged hydrogen structure also has been proposed by Hart[9] to account for products occurring in the acylation of cyclopropane.

Theoretical investigations of the geometry of $C_3H_7^+$ thus far have been based on semiempirical techniques on an order of complexity comparable to Hückel theory.[10] In addition to the well-known uncertainties inherent in such treatments, it has also been pointed out previously that ionic and charged molecules often show a behavior markedly different from that of neutral systems when the sum of near Hartree–Fock orbital energies is considered as a possible geometry determining quantity.[11]

Recently, it has become practicable to perform accurate *ab initio* SCF calculations on systems the size of $C_3H_7^+$. In this study such calculations are reported for a number of possible geometries of the ion leading to a reasonably well-defined energy minimum. All electrons are included in the treatment and the basis set is sufficiently large to give results within 0.008 au of the Hartree–Fock energy for the carbon atom.[12] Other applications of the techniques discussed here have previously been reported for a variety of polyatomic molecules.[11–16] The results obtained in the study are interpreted by considering the effect of an additional proton on calculated molecular orbitals of cyclopropane.[17] Charge density contour diagrams of certain molecular orbitals also are presented.

Calculations

The basis set employed in this work has been described previously in an application to the ethylene molecule where numerical values of all exponents and coefficients are tabulated.[12] Fixed groups, or linear combinations of Gaussian functions, are defined in terms of a fundamental basis set of single Gaussian functions, and lobe functions are used instead of spherical harmonic functions. Five-component p groups, plus three s groups, a three-component short range, a three-component long range, and a four-component intermediate range, are used for each carbon. A scaled five-component 1s function, $\eta = 1.414$, is used for each hydrogen and the proton. Molecular orbitals are expanded as linear combinations of the 25 fixed basis groups, and coefficients are determined by a SCF

(1) Author to whom inquiries should be addressed at the Department of Chemistry, State University of New York at Stony Brook, Stony Brook, N. Y. 11790.

(2) American Petroleum Institute, Research Project 44, "Catalog of Mass Spectral Data," Carnegie Institute of Technology, Pittsburgh, Pa., 1947–1956.

(3) M. B. Wallenstein, A. L. Wahrhaftig, and H. Eyring, "The Mass Spectra of Large Molecules. I. Saturated Hydrocarbons," Institute for the Study of Rate Processes, University of Utah, Salt Lake City, Utah, 1951.

(4) P. N. Rylander and S. Meyerson, *J. Am. Chem. Soc.*, 78, 5799 (1956).

(5) D. P. Stevenson and C. D. Wagner, *J. Chem. Phys.*, **19**, 11 (1951).

(6) R. L. Baird and A. A. Aboderin, *J. Am. Chem. Soc.*, **86**, 252 (1964).

(7) G. J. Karabatsos, C. E. Orzech, and S. Meyerson, *ibid.*, 87, 4394 (1965).

(8) A. A. Aboderin and R. L. Baird, *ibid.*, **86**, 2300 (1964).

(9) H. Hart and R. H. Schlosberg, *ibid.*, **88**, 5030 (1966).

(10) R. Hoffmann, *J. Chem. Phys.*, **40**, 2484 (1964).

(11) R. J. Buenker and S. D. Peyerimhoff, *ibid.*, **45**, 3682 (1966).

(12) J. L. Whitten, *ibid.*, **39**, 349 (1963); **44**, 359 (1966).

(13) R. J. Buenker, S. D. Peyerimhoff, L. C. Allen, and J. L. Whitten, *ibid.*, **45**, 2835 (1966).

(14) S. D. Peyerimhoff and R. J. Buenker, *ibid.*, **47**, 1953 (1967).

(15) S. D. Peyerimhoff, R. J. Buenker, and L. C. Allen, *ibid.*, **45**, 734 (1966).

(16) S. D. Peyerimhoff, R. J. Buenker, and J. L. Whitten, *ibid.*, **46**, 1707 (1967).

(17) R. J. Buenker, and S. D. Peyerimhoff, results to be published.

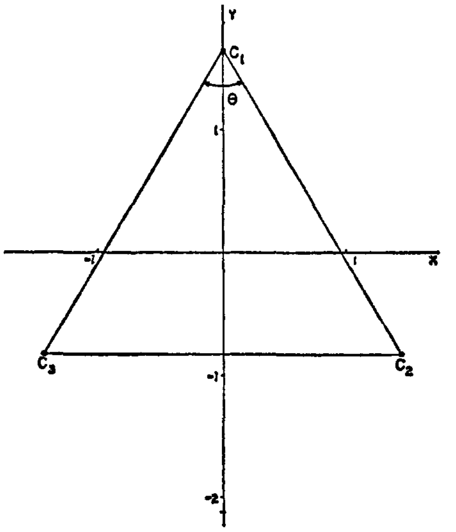

Figure 1. Equilibrium configuration of the carbon atoms in cyclopropane. The angle θ is varied in studies of ring opening.

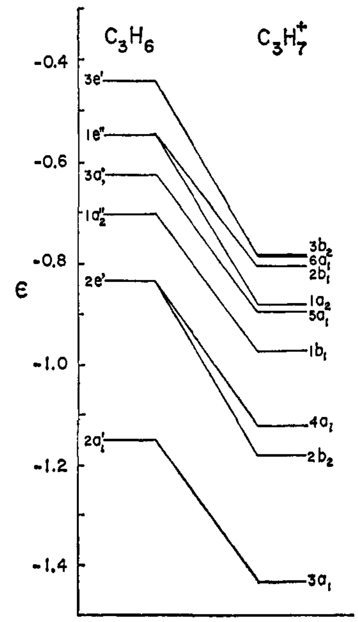

Figure 2. Valence orbital energy levels for C_3H_6 and $C_3H_7^+$ in their equilibrium geometries.

minimization of the total energy for each nuclear configuration.

In the first series of calculations, the nuclear framework of cyclopropane was held fixed at the experimental geometry shown in Figure 1, and the position of the proton was varied along the negative y axis (edge-protonated) and also along the z axis (face-protonated). The total energy, nuclear repulsion energy, and sum of orbital energies are listed in Table I for each case examined. From these results it is evident that the edge-protonated form is strongly favored, giving a maximum binding energy of 0.197 au relative to C_3H_6 for proton coordinates of (0, −2.90, 0).[18]

Table I. Proton Coordinates (x, y, z), Total Energy (E_T), Sum of Orbital Energies ($\Sigma\epsilon_i$), and Nuclear Repulsion Energy (V_N) for 60° $C_3H_7^{+a}$

(x, y, z)	E_T	$\sum_i \epsilon_i$	V_N
(0, −1.43, 0)	−116.76254	−44.69126	87.19415
(0, −1.83, 0)	−116.93411	−44.55169	86.07143
(0, −2.40, 0)	−117.08341	−44.25937	84.51624
(0, −2.70, 0)	−117.11009	−44.08758	83.80051
(0, −2.90, 0)	−117.11375	−43.97244	83.36897
(0, −3.00, 0)	−117.11239	−43.91237	83.16640
(0, −3.25, 0)	−117.10265	−43.76558	82.69617
(0, 0, 1.00)	−116.78950	−44.52664	86.87655
(0, 0, 2.00)	−116.95499	−43.93338	84.42654
(0, 0, 2.75)	−116.96414	−43.51049	82.96274
(C_3H_6)	−116.91636		75.73748

[a] Coordinates of carbon and hydrogen nuclei are given in Table II.

The possibility of ring opening is explored in a second series of calculations. The CCC angle θ, shown in Figure 1, is increased successively to 80, 100, and 120° with the relative geometry of CH_2 groups held fixed; planes containing the nuclei in CH_2 groups are taken to bisect the CCC angles to give over-all C_{2v} symmetry for each molecular geometry examined. Coordinates of all nuclei except the proton are given for each angle in Table II. Total energies, nuclear repulsion energies, and sums of orbital energies are given in Table III for each proton origin in the 80° series, and in Table IV for the 100 and 120° geometries, respectively. Minimum energy occurs in the 80° case at proton coordinates (0, −2.40, 0) with a binding energy of 0.247 au with respect to cyclopropane.

(18) All energies and coordinates given in this paper are in atomic units, 27.21 eV and 0.529 Å, respectively.

Two additional calculations are reported in Table III for distorted geometries in which the proton is moved from its equilibrium position 0.5 au in the x direction, $C_s(xy)$ symmetry, and 0.5 au in the z direction, $C_s(yz)$ symmetry. In both cases the energy is increased although the increase is much more significant for distortion out of the plane of carbon nuclei.

Bonding in Protonated Cyclopropane

Addition of a proton to the cyclopropane ring gives rise to two distinct effects. The first is a stabilization of all orbitals, as shown in Figure 2, caused by the presence of an additional attractive charge in the system. Inner-shell orbitals are omitted from the diagram, but these orbitals also exhibit the same dramatic stabilization in going from C_3H_6 to $C_3H_7^+$.

The second effect concerns interaction of molecular orbitals of proper symmetry with the proton basis function to give a_1 orbitals in the C_{2v} protonated form. In 60° cyclopropane, the highest energy orbital of such symmetry is one of the doubly degenerate 3e′ molecular orbitals which forms a CC bond composed essentially of $2p_x$ and $2p_y$ atomic orbitals. Figure 3 shows the approximate composition of this orbital and also of the next lowest molecular orbital of a_1 symmetry, the $3a_1'$. Analysis of the SCF vector calculated for the 80° equilibrium configuration case shows the proton coefficient to be largest in the 3e′ → $6a_1$ orbital with a value of 0.39. In the $5a_1$, $4a_1$, and $3a_1$ orbitals, coefficients are smaller at −0.11, 0.15, and 0.08, respectively. A charge-density contour diagram of the $6a_1$ molecular orbital is shown in Figure 4 illustrating the general features of the bridged hydrogen bond. A diagram for the $3a_1'$ → $5a_1$ orbital shown in Figure 5

Table II. Coordinates of Carbon and Hydrogen Nuclei in 60, 80, 100, and 120° Cases of $C_3H_7^+$

	60°	80°	100°	120°
C_1	(0, 1.6628, 0)	(0, 1.6628, 0)	(0, 1.6628, 0)	(0, 1.6628, 0)
H_a, H_b	(0, 2.6738, ±1.7511)	(0, 2.6728, ±1.7511)	(0, 2.6738 ±1.7511)	(0, 2.6738, ±1.7511)
C_2	(1.44, −0.8314, 0)	(1.8512, −0.5434, 0)	(2.2062, −0.1885, 0)	(2.4942, 0.2228, 0)
H_a, H_b	(2.3156, −1.3369, ±1.7511)	(2.7675, −0.9707, ±1.7511)	(3.1562, −0.5342, ±1.7511)	(3.4707, −0.0389, ±1.7511)
C_3	(−1.44, −0.8314, 0)	(−1.8512, −0.5434, 0)	(−2.2062, −0.1885, 0)	(−2.4942, 0.228, 0)
H_a, H_b	(−2.3156, −1.3369, ±1.7511)	(−2.7675, −0.9707, ±1.7511)	(−3.1562, −0.5342, ±1.7511)	(−3.4707, −0.0389, ±1.7511)

Table III. Proton Coordinates, Total Energy, Sum of Orbital Energies, and Nuclear Repulsion Energy for 80° $C_3H_7^+$ in C_{2v} and C_s Symmetry[a]

(x, y, z)	E_T	$\sum_i \epsilon_i$	V_N
(0, −1.2, 0)	−117.01855	−44.14015	81.91237
(0, −1.4, 0)	−117.06279	−44.09570	81.52235
(0, −1.8, 0)	−117.12967	−43.99163	80.71469
(0, −2.2, 0)	−117.16067	−43.86282	79.93181
(0, −2.4, 0)	−117.16353	−43.79226	79.56418
(0, −2.8, 0)	−117.15029	−43.64080	78.88845
(±0.5, −2.4, 0)	−117.16159	−43.79708	79.59890
(0, −2.4, ±0.5)	−117.10051	−43.57264	79.46781

[a] Coordinates of carbon and hydrogen nuclei are given in Table II.

Table IV. Proton Coordinates, Total Energy, Sum of Orbital Energies, and Nuclear Repulsion Energy for 100 and 120° $C_3H_7^+$[a]

(x, y, z)	E_T	$\sum_i \epsilon_i$	V_N
	100° Geometry		
(0, −0.188, 0)	−116.82370	−44.08083	80.28613
(0, −0.40, 0)	−116.88282	−44.00468	79.90253
(0, −0.60, 0)	−116.93052	−43.93621	79.55195
(0, −0.80, 0)	−116.97290	−43.87477	79.20382
(0, −1.50, 0)	−117.07368	−43.69864	77.99156
(0, −1.80, 0)	−117.09097	−43.62765	77.49363
(0, −2.00, 0)	−117.09441	−43.57883	77.17590
(0, −2.20, 0)	−117.09226	−43.52779	76.87167
	120° Geometry		
(0, 0.22, 0)	−116.61101	−43.98268	79.35998
(0, 0, 0)	−116.74150	−43.89054	78.74675
(0, −0.20, 0)	−116.81230	−43.81074	78.27846
(0, −0.40, 0)	−116.86052	−43.73392	77.85803
(0, −1.00, 0)	−116.94706	−43.53708	76.75511
(0, −1.40, 0)	−116.97520	−43.43677	76.10549
(0, −1.80, 0)	−116.98288	−43.34769	75.51457
(0, −2.20, 0)	−116.97420	−43.25774	74.98139

[a] Coordinates of carbon and hydrogen nuclei are given in Table II.

illustrates much less bonding tendency. The total charge density in the region of the bridged hydrogen bond is given in Figure 6.

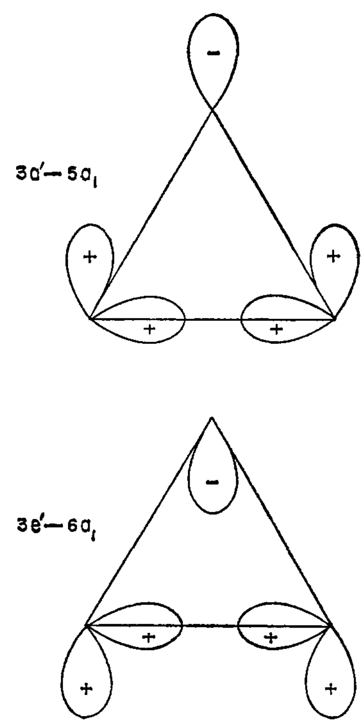

Figure 3. General features of the $3a_1' \rightarrow 5a_1$ and $3e' \rightarrow 6a_1$ molecular orbitals of cyclopropane.

Results obtained by opening the $C_3H_7^+$ ring are shown in Figure 7 where energies of valence orbitals calculated at optimum proton positions are plotted as a function of CCC angle. Inner-shell molecular orbitals, $1a_1$, $1b_2$, and $2a_1$, which are essentially linear combinations of carbon 1s orbitals, are not significantly affected by these angle variations. The lowest lying valence orbital is the $3a_1$ consisting of long-range s groups on each carbon plus a smaller amount of $2p_x$ character from carbons 2 and 3. A change in angle from 60 to 120° results in a greater s contribution from C_1 and the proton, but a decrease in interaction between the long-range s and $2p_x$ orbitals on C_2 and C_3 leads to a net decrease in stability.

The $2b_2$ molecular orbital which is mainly an antisymmetric combination of long-range s groups on C_2 and C_3 exhibits a stabilization with increased angle that can be attributed to a decrease in antibonding character with increasing distance between centers. The next orbital, $4a_1$, containing some proton character, shows a decrease in stability with increasing angle. This orbital is mainly a combination of long-range s, $2p_x$, and $2p_y$ functions representing bonds from C_2 and C_3 to C_1; opening the ring tends to remove $2p_y$ atomic orbitals from bonding and leads to a decrease in stability.

Of the molecular orbitals which involve $2p_z$ functions, the $1b_1$ and $2b_1$ show a decrease in stability with increasing angle. The $1b_1$, composed essentially of $2p_z$ functions on C_2 and C_3, loses stability as the distance between the p functions increases while the decrease in stability of the $2b_1$ is due to a weakening of the bond between the $2p_z$ on C_1 with the two attached hydrogens, apparently in favor of increased CH bonding at

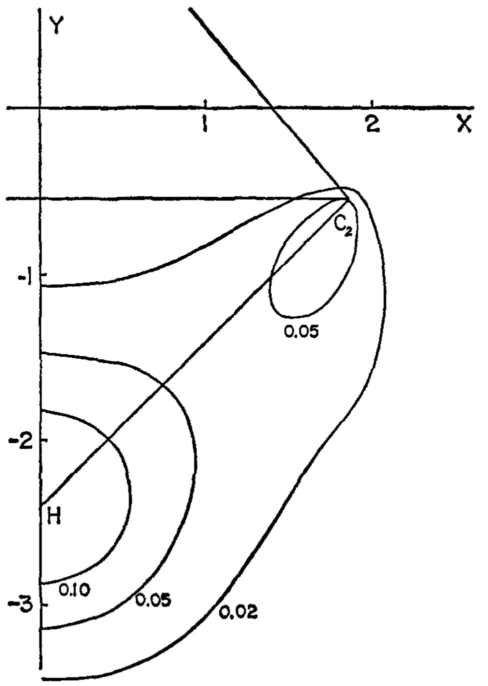

Figure 4. Charge density contour of the $6a_1$ molecular orbital of $C_3H_7^+$.

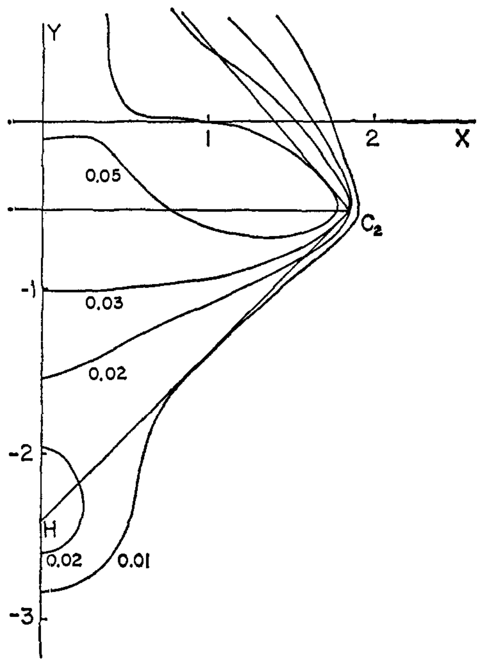

Figure 5. Charge density contour of the $5a_1$ molecular orbital of $C_3H_7^+$.

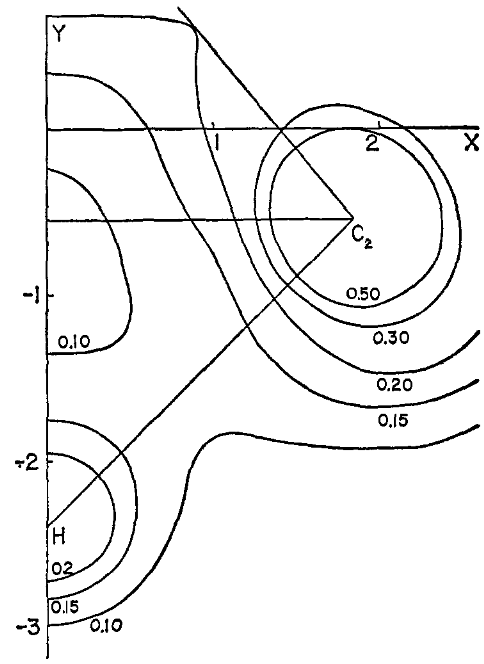

Figure 6. Total charge density contour of $C_3H_7^+$ in the region of the proton.

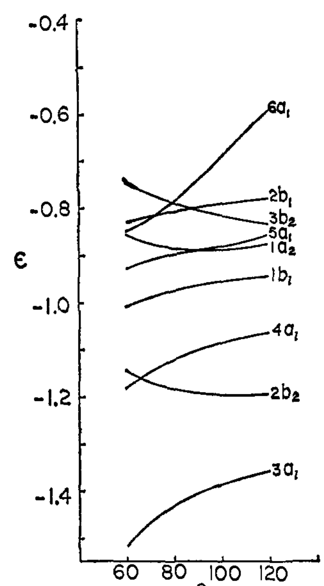

Figure 7. Valence orbital energies of $C_3H_7^+$ as a function of CCC angle, θ, with the proton in the position of maximum stability for each angle.

centers C_2 and C_3. The $1a_2$ molecular orbital is the third orbital involving $2p_z$ functions and is stabilized by an increase in angle which increases the distance between the antibonding lobes on C_2 and C_3. In general, the trends in the three above orbitals are to be expected; however, the magnitudes of the changes in stability are not large and do not have a major effect in determining the geometry of the molecule.

The $5a_1$ orbital would seem to be rather important at first since it is high lying and of proper symmetry to accommodate the proton, but the destabilization of this orbital is no greater than that of any other orbital encountered thus far. The orbital consists mainly of $2p_x$ and $2p_y$ functions as illustrated in Figure 3, and its decrease in stability is analogous to that of the $4a_1$ except for an increase in proton contribution with increase in angle.

The $6a_1$ is the highest molecular orbital which can interact with the proton basis function and in this respect is the most significant in determining the optimum angle of $C_3H_7^+$. As shown in Figure 7, the orbital undergoes a pronounced decrease in stability with increase in angle. This decrease can be attributed directly to a weakening of the bridged hydrogen bond caused by movement of carbon p function away from the bonding region. The sharpness of the decrease in

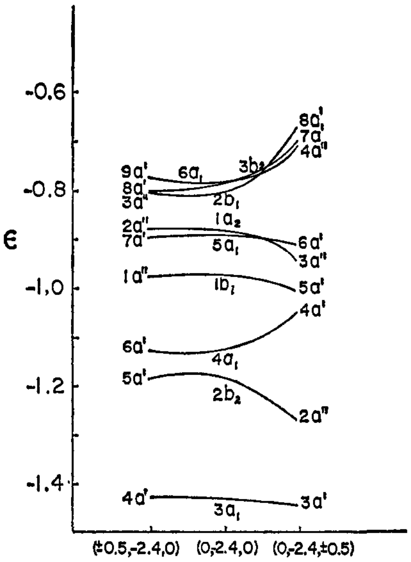

Figure 8. Valence orbital energies of $C_3H_7^+$ for equilibrium and distorted geometries.

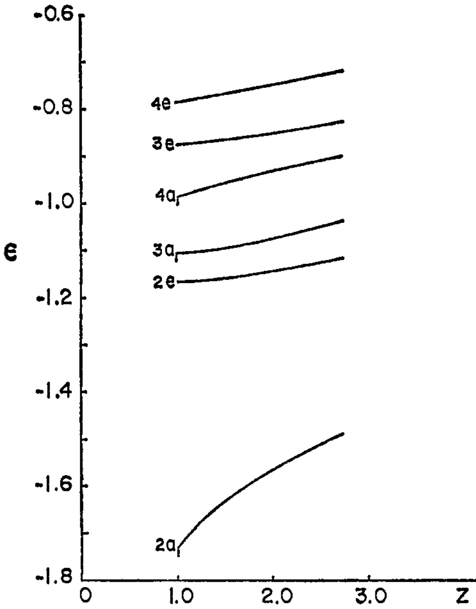

Figure 9. Valence orbital energies of face-protonated $C_3H_7^+$ as a function of proton z coordinate.

stability effectively rules out both 100 and 120° as possible optimum angles.

The highest molecular orbital, the $3b_2$, is stabilized by an increase in angle. Essentially, this orbital is a combination of $2p_x$ on C_1 and $2p_x$ and $2p_y$ functions on C_2 and C_3; increasing the angle causes stabilization by reducing the antibonding interaction between functions on centers 2 and 3.

Pursuing the orbital energy arguments outlined above would lead to a rationalization of an optimum angle of 60° since it is for this geometry that the sum of orbital energies (and the sum of valence orbital energies) is lowest and the bridged hydrogen bond orbital, $6a_1$, is most stable. The key point in understanding why in fact the 80° configuration is favored lies in a consideration of nuclear and electronic repulsion. The total energy of the system which of course is the geometry determining quantity can be expressed as

$$E = 2\sum_i \epsilon_i + (V_n - E_r)$$

where the summation is over all doubly occupied molecular orbitals with energy ϵ_i, and V_n and E_r are nuclear and electronic repulsion terms, respectively. As has been pointed out previously, angular variations in nonionic systems frequently result in changes in V_n sufficiently parallel to those in E_r such that $2\Sigma\epsilon_i$ shows a minimum near that of E. In $C_3H_7^+$, the nuclear repulsion increases by 3.8 au in going from 80 to 60°, but this increase is not completely offset by changes in E_r and as a result the calculated minimum E occurs at 80°. This conclusion clearly illustrates the need for establishing numerically significant changes in ϵ_i before advancing geometry predictions based on orbital energies, and in addition obviously suggests a criticism of geometry prediction from semiempirical theories which do not explicitly include effects of nuclear repulsion.

As the proton is moved toward the ring from its equilibrium position, there is an increase in proton coefficients in the lower lying a_1 orbitals, $3a_1$, $4a_1$, and $5a_1$, at the expense of the $6a_1$ as shown in Table V. This decrease in interaction with the molecular orbital that is best able to form a bridged-hydrogen bond, plus the effect of increased nuclear repulsion, is sufficient to establish an equilibrium configuration at somewhat greater distance from the ring than might be expected, at (0, −2.40, 0) au.

Table V. Proton Expansion Coefficients and Proton Coordinates for a_1 Valence Molecular Orbitals of 80° C_{2v} $C_3H_7^+$

(x, y, z)	$3a_1$	$4a_1$	$5a_1$	$6a_1$
(0, −1.2, 0)	0.241	−0.209	−0.268	0.308
(0, −1.4, 0)	0.206	−0.209	−0.254	0.318
(0, −1.8, 0)	0.144	0.193	−0.211	0.342
(0, −2.2, 0)	0.097	0.166	−0.146	0.375
(0, −2.4, 0)	0.080	0.151	−0.110	0.387
(0, −2.8, 0)	0.055	0.121	−0.054	0.399

A strong preference for location of the proton in the xy plane is indicated in Figure 8 which shows valence orbital energies for the equilibrium configuration and two distorted geometries involving displacements of the proton from equilibrium 0.5 au along x and z directions, respectively. In the latter nonplanar case, there is an extensive destabilization of the $6a_1 \rightarrow 7a'$ orbital showing that the planar p functions on carbon cannot bond satisfactorily with the proton unless it is in the xy plane as well.

As mentioned previously, face-protonated forms of $C_3H_7^+$ are calculated to be significantly less stable than the optimum side-protonated geometry although the $z = 2.0$ and 2.75 au cases reported in Table I are bound relative to C_3H_6. Figure 9 shows a plot of valence orbital energies *vs.* z coordinate of the proton. The sum of orbital energies is lowest at (0, 0, 1.0), but, for the same reasons noted earlier involving a lack of cancellation between nuclear and electronic repulsion, the proton is not bound for this geometry. Of the molecular orbitals available for combination with the proton basis function, only the $3a_1$ interacts significantly, and apparently this orbital is too low lying to bond effectively. A series of additional calculations also supports this point. In Table VI results are reported for $C_3H_7^+$ treatments in which molecular orbitals are constrained to be those of 60° cyclopropane although the Hamiltonian is for $C_3H_7^+$. Under such constraints the

Table VI. Results Obtained for Protonated Cyclopropane Using Molecular Orbitals Constrained to be Those of C_3H_6[a]

(x, y, z)	ΔV_N	ΔE_e	ΔE_T
Face-Protonated Geometry			
(0, 0, 0)	12.70257	−11.93554	0.76704
(0, 0, 1.0)	11.13906	−10.73843	0.40063
(0, 0, 2.0)	8.68906	−8.60077	0.08828
(0, 0, 2.5)	7.67287	−7.63338	0.03949
(0, 0, 3.0)	6.81470	−6.79396	0.02074
(0, 0, 3.5)	6.09338	−6.07949	0.01389
(0, 0, 4.0)	5.48697	−5.47573	0.01124
(0, 0, 5.0)	4.54219	−4.53329	0.00894
Edge-Protonated Geometry			
(0, −0.83, 0)	12.60680	−11.75292	0.85388
(0, −1.23, 0)	11.94670	−11.25986	0.68684
(0, −1.63, 0)	10.90718	−10.48114	0.42604
(0, −1.83, 0)	10.33396	−10.02938	0.30458
(0, −2.43, 0)	8.70003	−8.63534	0.06469
(0, −3.0, 0)	7.42892	−7.44728	−0.01836
(0, −3.5, 0)	6.53601	−6.57238	−0.03637
(0, −4.0, 0)	5.81256	−5.84859	−0.03603
(0, −4.5, 0)	5.22092	−5.25127	−0.03035

[a] ΔV_N = difference in nuclear repulsion energies of $C_3H_7^+$ and C_3H_6, ΔE_e = difference in electronic energies of $C_3H_7^+$ and C_3H_6, and ΔE_T = difference in total energies of $C_3H_7^+$ and C_3H_6.

proton never becomes bound in the C_{3v}, face-protonated case, but that in the C_{2v} edge-protonated case bonding occurs starting at a y coordinate of −3.0 au. Clearly, such calculations in which no polarization of C_3H_6 orbitals is allowed only establish upper bounds to total energies, but the significant point lies in the indication of a first-order difference in bonding ability at the two protonation sites.

Conclusions

The results of this study show that $C_3H_7^+$ in the gas phase is stable relative to C_3H_6 and that the equilibrium geometry corresponds to that of an edge-protonated species in which the proton is bonded to the ring by a bridged hydrogen bond. Bonding is due principally to an interaction of the proton with in-plane carbon 2p atomic orbitals of the $3e' \rightarrow 6a_1$ molecular orbital of cyclopropane and as such appears preferable to the $2p_z$ bonding above the ring required in the case of a face-protonated species. The proton strongly prefers to remain in the plane of carbon nuclei, and the increase in nuclear repulsion due to the proton is largely responsible for an opening of the ring to approximately 80° to give maximum stability. Variations in the nuclear and electronic repulsion contributions to the total energy are found to be important factors in determining the equilibrium geometry of this system, consequently ruling out the possibility of quantitative geometry predictions based solely on orbital energy calculations.

The question of rearrangement of $C_3H_7^+$ to give methyl cation and ethylene has not been explored explicitly in this study, but previous calculations on these systems[12,15] using comparable basis sets indicate that $C_3H_7^+$ is slightly lower in energy than the sum of ground-state energies of CH_3^+ and C_2H_4. Addition of an electron to give CH_3 and C_2H_4 is highly favorable energetically, however. The calculated edge-protonated geometry of $C_3H_7^+$ is in agreement with the proposed bridged hydrogen structure of protonated cyclopane intermediates in solution.

Acknowledgments. The authors thank Dr. Robert J. Buenker for his interest and helpful comments during the course of this work. Acknowledgment is made to the donors of the Petroleum Research Fund, administered by the American Chemical Society, for partial support of this research. The services and computer time made available to us by the Michigan State University Computer Laboratory have been invaluable in this study.